Charge Distribution and Crystalline Structure in Polyethylene Nucleated with Sorbitol

XIANG LI,[1] YI CAO,[1] QIANGGUO DU,[1] YI YIN,[2] DEMIN TU[2]

[1] Department of Macromolecular Science and the Key Laboratory of Molecular Engineering of Polymer, Fudan University, Shanghai 200433, China

[2] Department of Electrical Engineering, Xi'an Jiaotong University, Xi'an 710049, China

Received 30 August 2000; revised 8 January 2001; accepted 25 January 2001

ABSTRACT: The charge distribution in samples under direct current electrical field was measured by the pulsed electro-acoustic method, which showed that the space charges were greatly decreased and field distribution tended to be uniform in low-density polyethylene (LDPE) by adding 0.3 wt % bis-(*p*-ethylbenzylidene)sorbitol. The crystalline structures of LDPE and LDPE/sorbitol were studied. The non-isothermal crystallization kinetics were investigated by differential scanning calorimetry, which showed that sorbitol increases crystallization temperature and crystallinity, but lowers the Avrami exponent of crystallization. The results of wide-angle X-ray diffraction (WAXD) and small-angle light scattering (SALS) experiments show that the crystal form does not change, whereas the perfection of spherulites degrades in the presence of sorbitol. In addition to the obvious difference in crystalline morphology, observed by scanning electron microscopy, the spherulites in the LDPE/sorbitol sample are smaller in size and more in number than those of LDPE. It is well known that in semicrystalline polymers, impurities are expelled from crystalline regions into amorphous regions or interfaces of spherulites. The decrease of space charges can probably be attributed to the uniform distribution of impurities in the whole material, with smaller and imperfect spherulites. © 2001 John Wiley & Sons, Inc. J Appl Polym Sci 82: 611–619, 2001

Key words: charge distribution; polyethylene; Sorbitol; nonisothermal crystallization; SALS

INTRODUCTION

Polymers and polymer blends are frequently used as insulators in electric engineering. The insulation characteristic of polymers lies in many localized states in the energy band structure and accumulation of space charge. It is therefore important to understand the mechanism of formation and accumulation of space charge in power cable and to discuss the possibility of elimination. Polyethylene (PE) has been extensively used as an insulating material for power cables and communication cables because of its high resistivity and low tanδ. Many papers have been published on charge distribution and electrical conduction in the PE system.[1–4] It has been reported, for example, that the impulse breakdown strength of PE can be improved by blending with the ionomer[2] and ethylene-vinyl acetate copolymer (EVA).[4]

PE is a typical semicrystalline polymer. Its crystalline structure must affect the distribution of space charge. A few research works have been devoted to the relationship between charge distribution and crystalline morphology.[5, 6] However,

Correspondence to: Q. Du (qgdu@fudan.edu.cn).

Journal of Applied Polymer Science, Vol. 82, 611–619 (2001)

we are still far away from a complete understanding because of the complexity of crystalline structure, which includes crystallinity, the crystalline form, the size and perfection of spherulites, the thickness of crystalline lamellae, etc.

Sorbitol is a typical nucleating agent for polypropylene to improve its transparence, but only a few studies have been devoted to the low-density lipoprotein (LDPE)/sorbitol system. In this work 0.3 wt % of sorbitol was added to LDPE. The crystallization kinetics were compared with the virgin LDPE under nonisothermal conditions by the differential scanning calorimetry (DSC) method, and the relationship of the charge distribution and crystalline morphology was discussed with the aid of the pulsed electro-acoustic (PEA), small-angle light scattering (SALS), wide-angle X-ray diffraction (WAXD), and scanning electron microscopy (SEM) methods.

EXPERIMENTAL

Materials

LDPE was cable grade product DJ200 of Shanghai Petrochemical Company Ltd.. Bis-(*p*-ethylbenzylidene)sorbitol was obtained from Mitsui Toatsu Chemicals Inc., Japan, and was used as received.

Preparation of Samples

LDPE and 0.3 wt % sorbitol were mixed in the mixer of a Brabender Plasticorder at a rotor speed of 40 rpm and a temperature of 230 °C for 5 min. As a control, the virgin LDPE was subjected to the same processing. Films ~0.5 mm in thickness were prepared using a hot press at 170 °C for 5 min. These films were used for the measurement of PEA, WAXD, DSC, and SEM experiments.

Space Charge Measurement

The space charge distribution in samples was measured by the PEA method, as shown in Figure 1 [direct current (dc) source, 0–20 kV; pulse width, 20 ns; pulse voltage, 0–1 kV]. The diameter of copper electrode was 25 mm. Aluminum was deposited on two sides of plate samples as the electrodes. Silicone oil was used as an acoustic coupling agent to make a good acoustic contact between the sample electrode and the measure electrode. The principle of this method and details

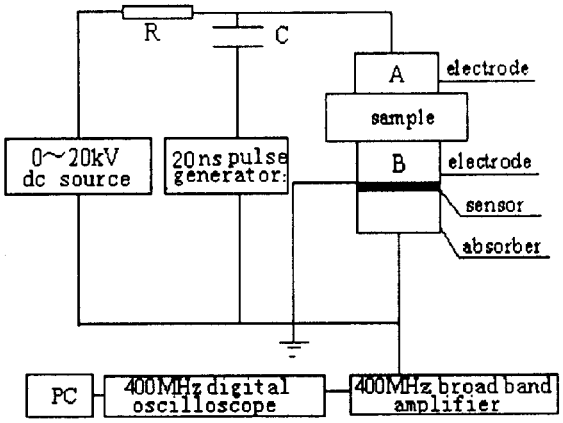

Figure 1 Schematic diagram of apparatus for measurement of sample space charge distribution.

of measurement were described in a previous paper.[7]

DSC Analysis

The crystallization kinetics of the samples were investigated under nonisothermal conditions.[8–11] A Perkin Elmer DSC-7 was used for the thermal analysis and data gathering. The sample was first rapidly heated up to 170 °C, ~60 °C higher than the melting point of LDPE, and maintained at this temperature for 5 min to erase any previous morphological history that the sample might be carrying. The sample then nonisothermally crystallized when it was cooled down to 0 °C at selected cooling rates of 2.5, 5, 10, and 20 °C/min. The entire process of crystallization was performed under nitrogen. The enthalpy of crystallization of 100% crystalline LDPE was reported as 68.2 cal/g,[12] and the degree of the crystallinity was calculated from the crystallization enthalpy of samples.

WAXD and SALS

WAXD measurements were carried out at room temperature on a diffractometer equipped with a CuK_α tube and Ni filter over a range of diffraction angle $2\theta = 5–40°$. The H_V light-scattering patterns were recorded on a SALS photometer equipped with a polarizer, an analyzer, and a He-Ne laser source.

Crystalline Morphology

The morphology of the samples was analyzed with a Hitachi S-520 scanning electronic microscope. The samples for morphology measurement

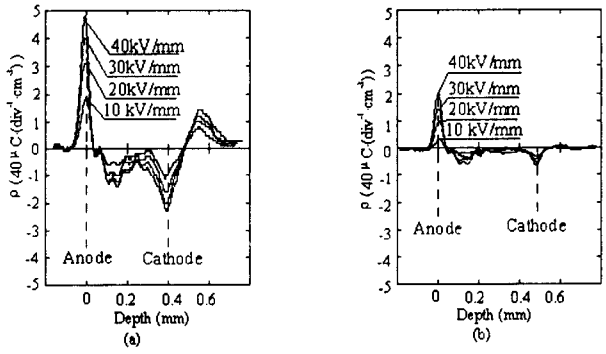

Figure 2 Charge distribution at various voltages of (a) LDPE and (b) LDPE/sorbitol.

were prepared by cryogenically fracturing the samples in liquid nitrogen. The amorphous regions were selectively extracted from these samples with toluene vapor.

RESULTS AND DISCUSSION

Charge distribution in LDPE and LDPE/sorbitol are shown in Figures 2 and 3. Figure 2 shows the charge distribution obtained while the dc voltages were being applied at the stresses of 10, 20, 30, and 40 kv/mm and Figure 3 shows the charge distribution after short circuit (discharging) for 10 s and 1, 10, 30, and 60 min. Under the dc voltages, the data in Figure 2 show the heterocharges in the samples of LDPE and LDPE/sorbitol. The peak of negative charges is much larger than that of positive charges, although the heterocharges appear in both samples, which is probably due to the neutralization. The charges in both samples increase to a different extent as the voltage increases; however, the density of charge in LDPE/sorbitol during charging is extremely small compared with pure LDPE. In general, the heterocharges in PE generate from chain ends, short branch chains, and impurities including initiator, peroxides, and metal irons generated in the course of synthesis and process.[3] As is shown in Figure 3, it is more interesting that almost no charge remained in LDPE/sorbitol after discharging as short as 10 s, whereas a few positive charges remained in pure LDPE. In terms of these phenomena, we can presume that considerable hopping sites or shallow traps must exist in LDPE/sorbitol, so that the charges formed during the charging step disappear easily to the electrodes on removal of the voltage. Because of the many deep traps in the pure LDPE, the charges once formed in the sample may not disappear easily after discharging.

To study the crystallization behavior under nonisothermal conditions, the Ozawa equation[9] was used to analyze the data. Ozawa assumes that crystallization occurs at a constant cooling rate and that crystallization originates from nuclei and grows as a spherulite with constant radial growth rate at a given temperature. The weight fraction of the crystallized material down to the temperature T is defined by eqs.1 or 2:

$$1 - X_T = \exp\{-K(T)/D^n\} \quad (1)$$

or

$$\log\{-\ln(1 - X_T)\} = \log K(T) - n \log D \quad (2)$$

where X_T is the fraction of material crystallized down to the temperature T; D is the cooling rate; $K(T)$ is the cooling function that is related to nucleation form, nucleation rate, growth rate, and so on; and n is the Avrami exponent obtained from the slope in the plot of $\log\{-\ln(1 - X_T)$ versus $\log D$ at a given temperature.

In this study, nonisothermal crystallization was conducted according to the method described in the Experimental section. Figure 4 shows the corresponding DSC thermograms for samples obtained at the cooling rate of 10 °C/min. Figures 5 and 6 show the DSC thermograms of LDPE and LDPE/sorbitol at several cooling rates, respectively. It is shown that crystallization of LDPE/sorbitol occurs at a higher temperature than that

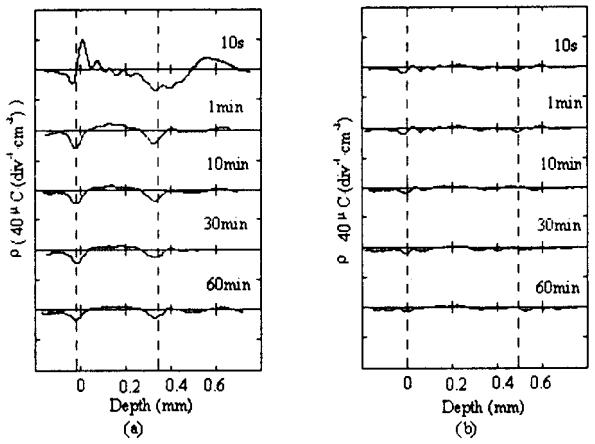

Figure 3 Charge distribution after short circuit of (a) LDPE and (b) LDPE/sorbitol.

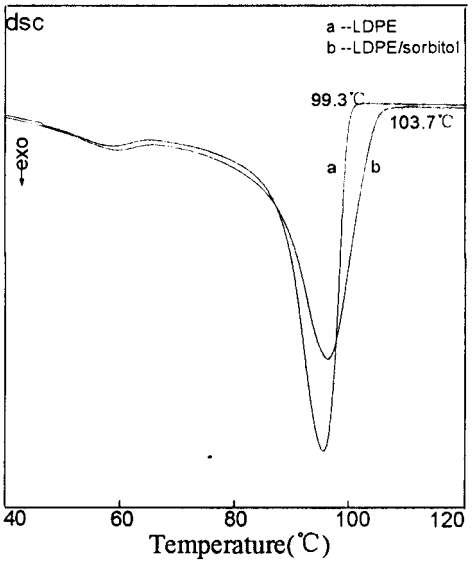

Figure 4 DSC thermograms of nonisothermal crystallization for LDPE and LDPE/sorbitol at the cooling rate of 10 °C/min.

of pure LDPE. The starting temperature of crystallization gradually lowers with increasing cooling rate for both samples. When cooling slowly, there is sufficient time to nucleate; therefore, the sample can crystallize at higher temperature. On the contrary, at faster cooling rate, the activation of nuclei occurs at lower temperature. In addition, the width of half-peak in DSC curve inversely relates to the perfection of crystal.[13] Because the

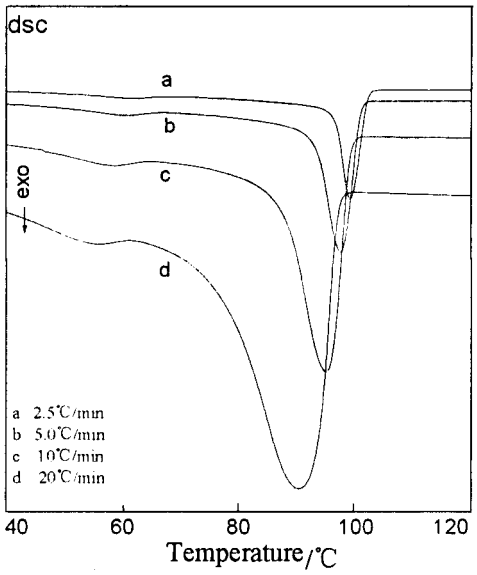

Figure 5 DSC thermograms of nonisothermal crystallization for LDPE for different cooling rates.

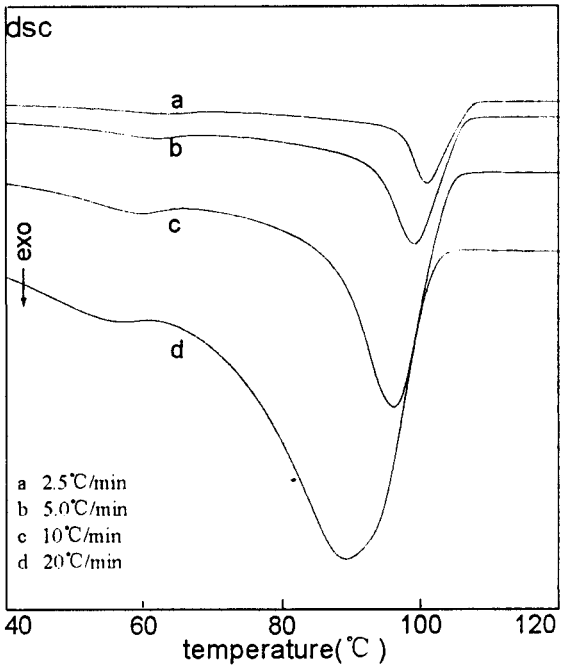

Figure 6 DSC thermograms of nonisothermal crystallization for LDPE/sorbitol for different cooling rates.

sample of LDPE/sorbitol shows wider peaks than LDPE at any cooling rate, the sample in the crystalline region must contain many more defects stemming typically from kinking, jogging, backfolding, and displacement of chains, from chain ends and from voids in space. When the cooling rate is low, the nonisothermal crystallization is similar to the isothermal crystallization at higher temperature. Crystallization proceeds at a slower rate, resulting in more perfect and stable crystals. As the cooling rate increases, supercooling becomes greater and more defective crystals are obtained. From the DSC curves, it is evident that secondary crystallization occurs at ~55 °C, especially at a high scanning rate. The secondary crystallization gives rise to more imperfect crystals around spherule surfaces because some segments of macromolecular chain in the amorphous regions can crystallize under low temperature.

The Avrami exponent n can also be determined from Ozawa plots and the slope of the plot of $\log\{-\ln(1 - X_T)\}$ versus $\log D$ by the least square method. In determination of the exponent, the crystalline weight fraction should be <0.5 because the effects of impingement, truncation of spherulites, and secondary crystallization kinetics might become very important at higher crystalline fractions, which may change the crystallization mechanism.[8, 14] The Avrami exponents so

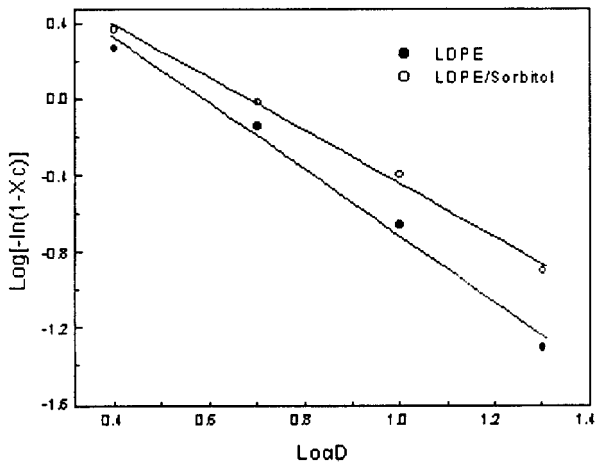

Figure 7 Plot of $\log[-\ln(1 - X_C)]$ versus $\log D$ for LDPE and LDPE/sorbitol at 85 °C.

obtained are plotted in Figure 7 and given in Table I. The value for LDPE/sorbitol is appreciably lower than that measured for neat LDPE. The measured Avrami exponent of LDPE agrees well with the literature data ($n = 1.72$).[15] These results confirm that the dispersed Sorbitol particles play a role of nucleating agent for the crystallization of LDPE and decrease supercooling temperature of the crystallization.

The value of Avrami exponent may be comprised of two parts: the contribution of the nucleation and the contribution of growth. The observed difference of the Avrami exponent may be essentially attributed to the nucleation of sorbitol. The Avrami exponent is close to 1 for LDPE/sorbitol and 2 for LDPE. The integral value of LDPE/sorbitol implies that it primarily forms one-dimensional crystallites from heterogeneous nucleation. Taking the considerable short-branching chains in LDPE into account, it is not difficult to understand that the value is lower compared with the number of dimensions of perfect spherulites. The short-branching chains are expected to be expelled from the crystal lattice and would effectively hinder crystal growth, giving rise to defects. As a result, the material would exhibit lower crystallinity.

The WAXD curves for the LDPE and LDPE/sorbitol samples are shown in Figure 8. Both samples have three principal crystalline reflection peaks at 2θ of 21.4, 23.7, and 36.1°, corresponding to the 110, 200, and 020 lattice planes of the orthorhombic crystalline form of PE, respectively. The amorphous scattering centered at $2\theta$of 19.8°. Reflections of a monoclinic or triclinic form are not seen on the X-ray diffractogram. These results show that sorbitol does not change crystal form. Interplanar distances shown in Table II are calculated by the Brag equation. Only a little difference was found for the two samples. The width of crystal peaks in WAXD crystallograms is inversely related to crystallite breadth perpendicular to the crystal plane.[16] Because the sample of LDPE/sorbitol shows wider peaks than LDPE, especially 200 (see Figure 8), the effect of sorbitol is not only a decrease in the average size of the crystallites, but also a decrease in the order of oriented macromolecular. These changes in the crystal structure are in good agreement with the results observed by the SEM and SALS (vide infra).

A light scattering method was used to investigate the crystalline superstructure occurring in the polymer film. The H_V scattering gives the familiar four-leaf-clover-type pattern, with its maximum intensity at the position angle (μ) of 45° and at a particular scattering angle (θ), which is inversely related to the size of spherulite.[17] The perfection of the spherulite decreases as the degree of diffusion of the four-leaf-clover-type struc-

Table I The Half-Peak Width, Avrami Exponent, and Crystallinity from DSC Thermograms at the Cooling Rate of 10°C min^{-1}

	LDPE				LDPE/Sorbitol			
Parameter	2.5°C min^{-1}	5°C min^{-1}	10°C min^{-1}	20°C min^{-1}	2.5°C min^{-1}	5°C min^{-1}	10°C min^{-1}	20°C min^{-1}
Half-peak width of DSC peak (°C)	3.5	5.2	7.5	14.7	6.2	8.5	11.5	21.0
Avrami exponent	—	—	1.79	—	—	—	1.35	—
Crystallinity from DSC (%)	—	—	42.0	—	—	—	37.8	—

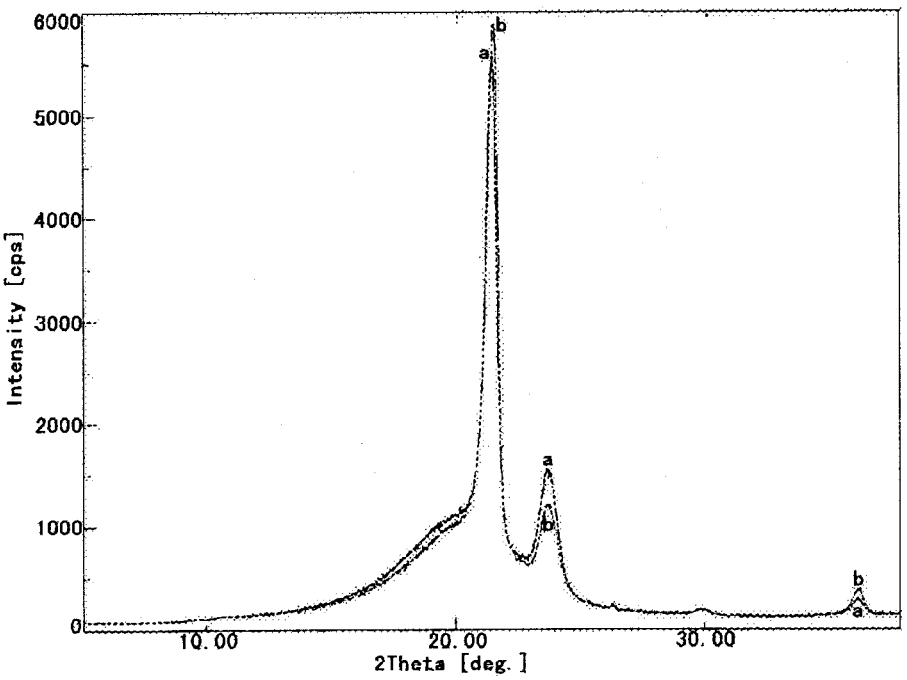

Figure 8 WAXD diffractograms of (a) LPDE/sorbitol and (b) LDPE.

ture increases. The theories of spherulitic scattering have been developed based on a model[18] of a homogeneous anisotropic sphere embedded in the isotropic medium, and the H_V scattering intensity of spherulite can be written as shown in eq. 3. This approach has successfully described the principal feature of most experimental patterns from spherulitic systems.

$$I_{H_V} = AV_S^2\left(\frac{3}{U^3}\right)^2\left[(\alpha_t - \alpha_r)\cos^2\frac{\theta}{2}\sin\mu\cos\right.$$
$$\left.\times\ \mu(4\sin U - U\cos U - 3SiU)\right]^2 \quad (3)$$

where H_V is scattering with vertical polarizer and horizontal polarization analyzer, α_r is the radial polarizablity, α_t is tangent polarizablity, θ is the scattering angle, μ is the position angle, V_S is the volume of the spherulite, and U is the shape factor and has the form

$$U = \frac{4\pi R_S}{\lambda}\sin\frac{\theta}{2} \quad (4)$$

$$SiU = \int_0^U \frac{\sin x}{x}\,dx \quad (5)$$

where R_S is the radius of the spherulite.

The dependence of scattering intensity on the position angle stems from the dependence of $3/U^3(4\sin U - U\cos U - 3SiU$ on the value of U. There is a maximum of scattering intensity in the scattering profile when U has the value of ~4.0,

Table II d-Spacing of Crystal Planes from WAXD Analysis of LDPE and LDPE/Sorbitol

	Crystal Plane				
Sample	110	200	020	210	011
LDPE	4.1487	3.7511	2.4833	2.9898	2.2619
LDPE/Sorbitol	4.1526	3.7604	2.4847	2.9917	2.2554

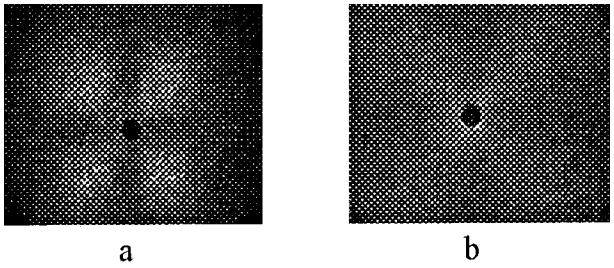

Figure 9 SALS patterns of (a) LDPE and (b) LDPE/sorbitol.

and the corresponding scattering angle is θ_m. The radius of the spherulite can be obtained with eq. 6:

$$4\pi\left(\frac{R_S}{\lambda}\right)\sin\frac{\theta_m}{2} = 4.0 \tag{6}$$

The scattering vector has the following form:

$$q = \frac{4\pi}{\lambda}\sin\frac{\theta}{2} \tag{7}$$

Then, the relation between the scattering vector and spherulite size can be written as eq. 8, and the size of spherulite can be roughly calculated with the measured value of q_m:

$$q_m R_S = 4.0 \tag{8}$$

The SALS profiles are obtained from the scattering of intensity (I) of spherulite versus the scattering vector (q) at a certain position angle $\mu = 45$ °C. The SALS patterns and profiles are shown in Figures 9 and 10, respectively. The crystals appear as spherulite and the size of the LDPE is larger than that of the LDPE/sorbitol. Another fundamental difference between the crystals is that the scattered intensity in Figures 9(a) and 10(a) passes through a maximum, whereas that in Figures 9(b) and 10(b) decreases continuously with the increase of scattering angle θ. The results show that the imperfection of the spherulites becomes more obvious in LDPE/sorbitol and that spherulite exhibits some perfection in the LDPE sample for the existence of a peak. In general there is one way to interpret these phenomena.[17] The interpretation is based on the possibility that the structure is uniformly composed of a single entity (i.e., spherulites). The average contour of the spherulite is considered to scatter light at small angles, whereas internal heterogeneities

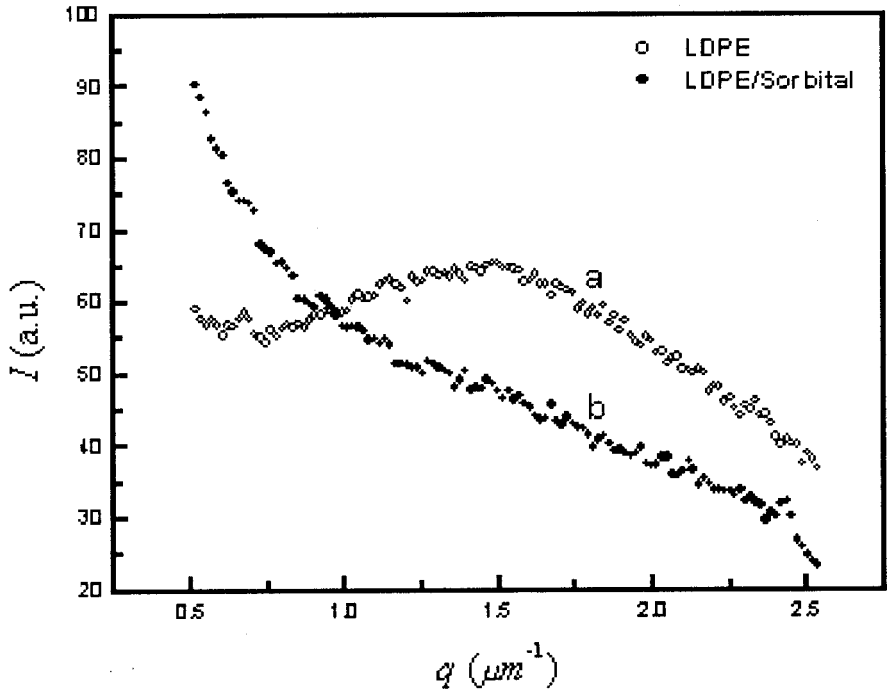

Figure 10 SAXS profiles of LDPE and LDPE/sorbitol. Intensity was plotted against the scattering vector q.

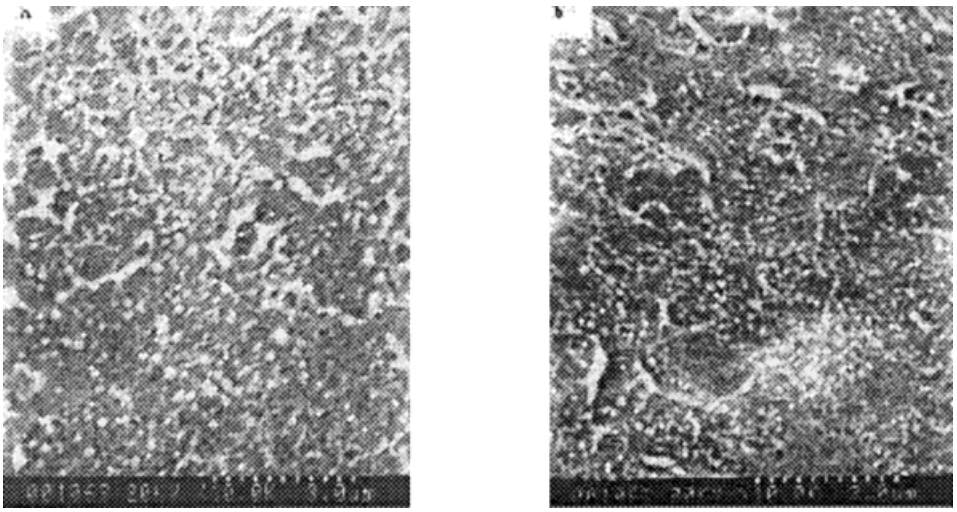

Figure 11 SEM patterns of (a) LDPE and (b) LDPE/sorbitol.

of the spherulites are considered to scatter light at high angles. The heterogeneities are believed to arise from the existence of the crystalline fibrils, which are not parallel to the radical direction of the spherulites but randomly assembled inside the spherulites. In Figure11, The SEM micrographs show the crystalline regions (white sections) that are left after the amorphous regions (gray sections) were etched by toluene vapor (the total length of the bar equals 3 μm). It should be noted that the amorphous regions were overetched by toluene vapor and the deeper-layer spherulites have partially appeared. The morphologic difference between samples can be determined directly: Spherulites of LDPE/sorbitol are smaller in size and much more in number than those of LDPE, and the average crystallite sizes are $\sim$0.2 and $\sim$0.3 μm, respectively. These results provide direct evidence that sorbitol particles act as a nucleating agent and decrease the imperfection of the spherulites.

The semicrystalline polymers, like PE, generally have a biphasic structure: crystalline and amorphous phases. The defects in the crystalline phase have similar characteristics to those of the amorphous phase. When polymer is applied to a high electrical field, an electron has to traverse amorphous and crystalline regions that behave differently with respect to the transport mechanism. Crystalline regions have a resistivity to charges because the molecular chains array in a compact and orderly manner. In contrast, amorphous regions have a strong affinity for charges not only because chains array in a loose and disorderly manner, but also all the impurities (including free radical residuals, peroxides, ions, and double bonds) almost disperse in amorphous phase, especially in the defects and interfaces of spherulites. Meanwhile, amorphous regions constitute the continuous phase in which the random chain can pass the charges on to the neighbor chain by changing its configuration. Hence, the charge distribution may depend strongly on the microstructure of the polymeric morphology.

The results of the PEA method indicate that charge distribution in LDPE/sorbitol is uniform during charging and no charge remains in the bulk after discharging. These results can be interpreted as indicating that LDPE/sorbitol contains many hopping sites and shallow traps. The hopping sites extend the mean free path of charges to enable subsequent charges to travel the entire material freely and reduce the charge accumulation in a partial locality. Combined with the analysis of crystalline morphology, we can use these results to conclude that the generation of considerable hopping sites relates directly to the presence of considerable defects in crystalline structure. So, the improvement of charge distribution in LDPE/sorbitol is attributed to two effects: decreasing the size of spherulite as well as slightly increasing the crystallinity causes the augmentation of the interfacial area between crystalline and amorphous regions and results in the improvement of the impurity distribution. The direct result is that, in a partial locality, the densities of the impurity and charge trap decrease. Second, considerable impurities and charges also can disperse in the crystalline regions because of the existence of defects. Consid-

erable defects and impurities, acting as hopping sites in the process of charge recombination, contribute to disappearance of the injected charges.

CONCLUSIONS

In the present report we measured the charge distribution of LDPE and LDPE/sorbitol and studied the crystallization process under nonisothermal conditions and crystalline morphology. We also investigated the microstructure of spherulites and interpreted the distinction between the two samples in terms of light scattering theories. From the results, the following conclusions can be made:

1. The charge distribution of LDPE can be obviously improved in the presence of sorbitol.
2. Sorbitol, acting as a nucleating agent for LDPE, changes the crystallization mechanism and decreases the perfection of the crystalline region as well as the inside of spherulites. The defects may cause the uniform distribution of impurities in the whole materials, with smaller and imperfect spherulites, and cause the decrease of space charge. However, there is no change in the crystalline form between LDPE and LDPE/sorbitol.
3. The improvement of the charge distribution in LDPE/sorbitol may be attributed to the existence of defects in the crystalline region as well as the inside of spherulites may cause

The work was supported by the Key Laboratory of Molecular Engineering of Polymer, Ministry of Education in China. Professor Tu wishes to thank Natural Science Fund Committee.

REFERENCES

1. Kitagawa, K.; Sawa, G.; Ieda, M. Jpn J Appl Phys 1980, 19, 389.
2. Suh, K.S.; Hwang, S.J.; Lee, C.R. IEEE Trans Dielec Elec Insul 1997, 4, 58.
3. Suh, K.S.; Koo, J.H.; Lee, S.H.; Park, J.K. Takada, T. IEEE Trans Dielec Elec Insul 1996, 3, 153.
4. Suh, K.S.; Kim, J.Y.; Lee, C.R.; Takada, T. IEEE Trans Dielec Elec Insul 1996, 3, 201.
5. Fan, Z.H.; Yoshimura, N. IEEE Trans Dielec Elec Insul 1996, 3, 849.
6. Kolesov, S.N. IEEE Trans Dielec Elec Insul 1980, 15, 382.
7. Li, Y.; Yasuda, M.; Takada, T. IEEE Trans Dielec Elec Insul 1994, 1, 188.
8. Lopez, L.C.; Wilkes, G.L. Polymer 19989, 29, 106.
9. Ozawa, T. Polymer 1971, 12, 150.
10. Kozlowski, W. J Polym Sci, Part C 1970,38, 47.
11. Eder, M.; Wlochowicz, A. Colloid Polym Sci 1983, 261, 621.
12. Wunderlich, B.; Cormier, C.M. J Polym Sci, Part A-2 1967, 5, 987.
13. Gupta, A.K.; Purwar, S.N. J Appl Polym Sci 1984, 29, 1595.
14. Eder, M.; Wlochowicz, A. Polymer 1983, 24, 1593.
15. Gupta, A.K.; Rana, S.K.; Deopura, B.L. J Appl Polym Sci 1994, 51, 231.
16. Yoda, O.; Odajima, A. Jpn J Appl Phys 1980, 19, 1241.
17. Hashimoto, T.; Murakmi,Y.; Okamori, Y.; Kawai, H. Polym J 1974, 6, 554.
18. Stein, R.S.; Rhodes, M.B. J Appl Phys 1960, 31, 1873.